CANM
ACMN

BOOK OF ABSTRACTS

Canadian Association of Nuclear Medicine

l'Association canadienne de médecine nucléaire

&

l'Association des médecins spécialistes en médecine nucléaire du Québec

May 5 -8, 2010 / du 5 au 8 mai 2010

Montréal, Québec

001

A NEW APPROACH TO TIME-BASED BONE MINERAL DENSITY DIFFERENCES

Lin Ling
Radiology, Faculty of Medicine, Memorial University of Newfoundland

Objectives: The purpose of this study is to calculate and apply total detectable difference (TDD) of bone mineral density (BMD) from longitudinal measurements, where TDD includes same-day machine error and long-term biological variation of individual patient's bone density, to reduce the overestimation of significance of BMD differences known to occur using least significant change (LSC).
Methods: A sample size of 5359 to 5533 females and males, aged 18 to 103 years old, having three sequential BMD studies over an average period of 7 years, was identified. Ordinary least squares linear regression was applied to each patient's serial BMDs to find scaled standard deviations and these deviations were used to create frequency distribution histograms, which, in turn, were fitted with half-normal distributions. TDD was then defined as 2SD for an approximate 95% confidence interval.
Results: Females and males have statistically indistinguishable TDD values allowing the results to be grouped. The TDD values of the combined female and male group are 0.042 for total hip, 0.047 for femoral neck, 0.059 for lumbar spine L1-L4 and 0.063 g/cm^2 for L2-L4 (see Table). Use of TDD reduced the frequency of detecting differences in BMD by approximately one-half.
Conclusions: TDD should be used to replace LSC because LSC does not account for natural patient's biological variation in BMD over time.

Support Information:

Total detectable difference (TDD) of bone density in g/cm^2 from female, male and female+male groups.

3 samples	Female			Male			Female + Male		
	n	TDD	R^{2*}	*n*	TDD	R^{2*}	*n*	TDD	R^{2*}
Total hip	5020	0.042	0.998	339	0.042	0.982	5359	0.042	0.997
Femoral neck	5138	0.047	0.996	345	0.051	0.969	5483	0.047	0.995
L1-L4	5146	0.059	0.997	348	0.061	0.983	5494	0.059	0.998
L2-L4	5183	0.062	0.997	350	0.066	0.985	5533	0.063	0.997

R^{2*} is the adjusted coefficient of determination of half-normal distribution fits to frequency histograms.

002

ROLE OF MYOCARDIAL PERFUSION IMAGING IN DETECTION OF OCCULT CORONARY ARTERY DISEASE IN HIGH RISK ASYMTOMATIC INDIVIDUALS

Dr Shazia Naseem, Dr Shagufta Quereshi.
Nuclear cardiology, Department of Nuclear Medicine, NORI hospital, Pakistan.

The **aim** of this study was to evaluate the role Exercise Tolerance Test (ETT) and Myocardial Perfusion Imaging (MPI) in the detection of occult coronary artery disease (CAD) in high-risk asymptomatic individuals.
Material and Methods: 25 individuals were enrolled in the study with one or more cardiac risk factors. Framingham scoring was used to classify as low, intermediate and high-risk group. ETT was categorized as normal, ischemic or

equivocal, on MPI perfusion defects were classified as normal, mild, moderate or severe degree defects, by 17-segment scoring system and 18 patients underwent coronary angiography.
Results: On assessment (n=25) intermediate risk group (n=14), low risk (n=7) and high risk (n=4) for CAD. Positive ETT (n=11) and (n=2) developed symptoms of angina during exercise; ischemic changes (n=9), equivocal response (n=2) and normal ECG response was seen (n=14). Semi quantitative analysis of scans (n=25) showed that normal perfusion scans (n=9), mild defect (n=4) and moderate to severe defect (n=12). On angiography vascular narrowing (n=15), normal angiograms (n=3). For patients in intermediate risk group (n=14), ischemic changes during ETT (n=6), perfusion defects on scan (n=10) and positive angiogram (n=10). In high-risk group (n=4), ETT positive (n=2) and perfusion defect (n=3) on scan, positive angiogram (n=3). In low risk group (n=7), 3 ETT positive (n=3) and MPI positive (n=3), and positive angiogram (n=2). Statistical analysis was done considering angiography as gold standard and it was found that
Conclusion: MPI is better diagnostic modality than ETT in diagnosis of occult coronary artery disease, in both intermediate and high risk group. MPI should act as a "gatekeeper" for invasive procedure in these groups.

003

ALTERED HEPATIC METABOLIC ACTIVITY IN PATIENTS WITH HEPATIC STEATOSIS ON FDG PET/CT

Abikhzer, Gad MD, CM, Alabed, Yazan Z. MD, CM, PhD, Azoulay, Laurent PhD, Assayag, Jonathan, BSc, Rush, Chris MD, CM, FRCPC.
Department of Nuclear Medicine, Jewish General Hospital, McGill University

^{18}F-Fluorodeoxyglucose (^{18}F-FDG) Positron emission tomography (PET) studies frequently use the liver as an internal reference organ to assess the significance of FDG uptake in pathological processes involving other organs. The purpose of this study was to assess if hepatic steatosis (HS) has a significant effect on the standardized uptake value (SUV) of the liver.
Methods: This prospective case control study analyzed ^{18}F-FDG PET/CT scans of patients with HS on the unenhanced CT portion of the study. SUVmax (corrected for both body weight and lean body mass) values in 37 patients with HS were compared to 37 control patients without HS.
Results: Patients with HS had statistically significant smaller mean values than the control subjects for the 1) liver SUVlbm (1.91 (SD: 0.57) vs. 2.17 (SD: 0.36), 2) the SUVlbm liver: mediastinum ratio (1.23 (SD: 0.19) vs. 1.35 (SD: 0.19)) and 3) the SUVbw liver: mediastinum ratio (1.24 (SD: 0.16) vs. 1.39 (SD: 0.22)).
Conclusion: HS results in a statistically significant small decrease in hepatic metabolic activity as measured by ^{18}F-FDG PET. However, as the degree of change is small, this decrease compared with normal controls is unlikely to have any clinical significance on the use of the liver as an internal reference organ for the interpretation of ^{18}F-FDG PET scans.

004

THE INAPPROPRIATENESS OF THE SUM OF EXPONENTIAL TERMS FOR MODELLING PLASMA CONCENTRATIONS OF BOLUS-INJECTED, RADIOLABELED DTPA

C. A. Wesolowski[1], R. C. Puetter[2, 3], P. S. Babyn[4], and Lin Ling[1]
[1] Memorial University of Newfoundland, St. John's, Newfoundland, Canada, [2] University of California, San Diego, La Jolla, California, USA, [3] Pixon Imaging LLC, San Diego, California, USA, [4] The Hospital for Sick Children, University of Toronto, Toronto, Ontario, Canada

Objectives: Four statistical tests were applied to explore the problems in estimating plasma clearance (CL ml/min) using Sums of (n) Exponential Terms (E_n SETs) fit to marker concentration of bolus-dilution of ^{169}Yb-DTPA (n=41, 8 samples, 10-240 min) and ^{99m}Tc-DTPA (n=5, 9 samples, 5-180 min).

Methods: Test 1 characterized E_2 SET's parameter estimation error using bootstrap. Test 2 explored sample-subset selection effects on E_1 and E_2 SET parameters. Test 3 explored E_2 SET goodness-of-fit testing. Test 4 examined E_2 SET extrapolative errors.
Results: Test 1 found that 19/46 E_2 elimination rate constants' confidence intervals included 0, implying that the complexity of $E_{n>1}$ models was statistically unjustified. In Test 2, the standard deviation of residuals changed with sample-subset selection and was >3%, the maximum expected relative measurement error. Further, 8.1% of E_2 fit attempts yielded degenerate E_2 fits. Test 3 found the magnitude of the E_2 models' mean residuals failed *t*-testing for 6 of the 8 sample times. For all samples, Chi-squared testing of fit quality suggested poor fits ($P<0.039$, $n=46$). Test 4, extrapolation, showed significant underestimation of concentration over time (31/46 times, Wilcoxon signed-rank sum $P=0.0035$) and overestimation of CL.
Conclusions: Consequently, SETs for modeling DTPA concentration are inappropriate and need replacement by better models.
Supporting Information:

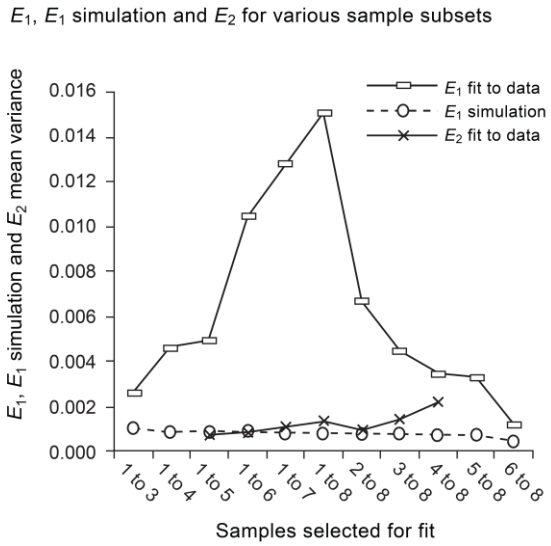

This Figure shows that the mean variances from E1 and E2 models are instable with respect to the choice of subsets from the 8 samples of the 41 patients.

005

LIMITATIONS OF ORDINARY LEAST SQUARES FITTING OF GAMMA VARIATE FUNCTIONS TO PLASMA-CLEARANCE CURVES

Carl A Wesolowski,[1] Richard C Puetter,[2, 3] Paul S Babyn,[4] and Lin Ling[1]
[1] Memorial University of Newfoundland, St. John's, Newfoundland, Canada. [2] University of California, San Diego, La Jolla, California, USA. [3] Pixon Imaging LLC, San Diego, California, USA. [4] The Hospital for Sick Children, University of Toronto, Toronto, Ontario, Canada.

Objectives: For ^{169}Yb- and ^{99m}Tc-DTPA chelates and 46 bolus-dilution curves, the limitations of the ordinary least squares (OLS) gamma variate (GV) model for plasma clearance (CL) and volume of distribution (V) were explored using four tests:
Methods: (i) fit parameter variability using bootstrap, (ii) fit parameter sensitivity to fits to subsets of the data, (iii) goodness-of-fit, and (iv) extrapolation accuracy.

Results: These tests showed: (i) the precision of CL and V from GV is better (P<0.0001) than those from the sum of two exponential terms (E_2); (ii) the GV fit easily converges irrespective of sample-subset choice, constraints or OLS regression technique; (iii) for progressively later-time samples, the GV models' unacceptably high frequency of CL=0 results greatly improved and the curve-fitting error decreased such that when only the latest samples from hours 1 to 4 were fit the mean error became insignificant (t-test P=0.87-0.99), whereas E_1 models could not accurately fit the early or late-time behaviour (P=0.030-0.032, hours 2 to 4, n=41); (iv) finally, extrapolation of bolus-dilution was good for constrained GV fits (Wilcoxon signed-ranks sum P=0.76), but poor (P=0.007) for constrained E_2 fits.
Conclusions: Unfortunately, however, although the GV function well describes the late bolus-dilution curve, OLS extraction of CL values was unreliable.

Supporting Information:

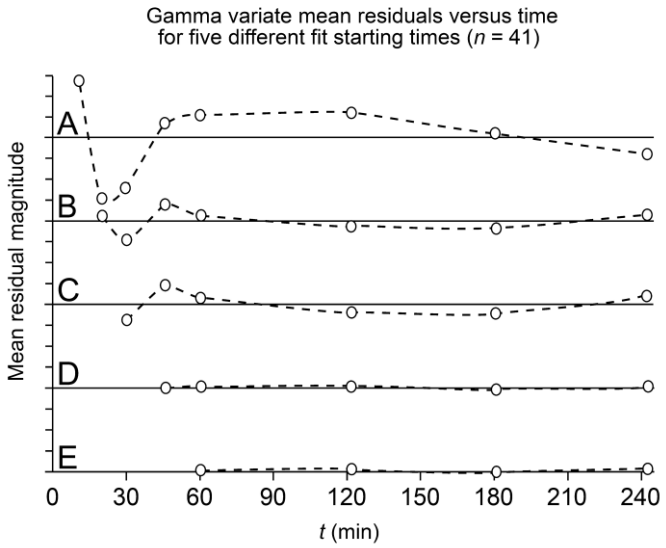

This figure shows the GV model performs the best when later-time sample (later than 45 minutes) are used.

006

TIKHONOV REGULARIZED GAMMA VARIATE FITS TO RADIOCHELATED-DTPA BOLUS-DILUTION CURVES WITH MINIMUM PLASMA-CLEARANCE RELATIVE ERROR

Carl A Wesolowski,[1] Richard C Puetter,[2, 3] Lin Ling,[1] and Paul S Babyn[4]
[1] Memorial University of Newfoundland, St. John's, Newfoundland, Canada, [2] University of California, San Diego, La Jolla, California, USA, [3] Pixon Imaging LLC, San Diego, California, USA, [4] The Hospital for Sick Children, University of Toronto, Toronto, Ontario, Canada.

Objectives: The Tk-GV model fits **G**amma **V**ariates to data by **Tik**honov regularization with shrinkage constant, λ, chosen to minimize the relative error in plasma clearance, CL (ml/min).
Methods: Four statistical tests explored Tk-GV **fits to bolus-dilution of ^{169}Yb-DTPA (n=41, 8 samples, 10-240 min) and ^{99m}Tc-DTPA (n=5, 9 samples, 5-180 min), with** comparison to one and two exponential term (E_1 and E_2) models with respect to: (1) physicality of ranges of model parameters, (2) effects on parameter values when different subsets of the data are fit, (3) characterization of Tk-GV residuals, and (4) extrapolative error and agreement with published correction factors.

Results: Test 1 showed the GV power function exponent to be $0.59<\alpha<0.99$, $n=46$, where $\alpha=1$ corresponds to CL=0 and no late-time concentration gradient between plasma and interstitium. Test 2 showed that the Tk-GV model is useful with 4 or more samples drawn between 5-10 minutes to 3-4 hours. Test 3 showed CL and λ to vary inversely. Test 4 showed $CL_{Tk\text{-}GV}$ clearance values did not need correction, agreed with published plasma clearance corrections to within 1 ml/min/1.73 m^2 and 0.6% with the general result that $CL_{E1}>CL_{E2}>CL_{Tk\text{-}GV}$ and finally that
Conclusions: $CL_{Tk\text{-}GV}$ were considerably more robust, precise and accurate than CL_{E2}, and should replace the use of CL_{E2}.

Supporting Information:

The performances of E2, GV and TK-GV models from the Wilcoxon test.

Fit type	Wilcoxon test probability	Median difference [a]	Median difference 95% confidence limits
E_2	0.0046	-0.0383	-0.0634 to -0.0140
E_2 [b]	0.0071	-0.0373	-0.0629 to -0.0118
GV	0.2446	0.0131	-0.0088 to 0.0491
GV [c]	0.7638	0.0039	-0.0158 to 0.0334
Tk-GV	0.9087	-0.0011	-0.0192 to 0.0217

[a] From Wilcoxon signed-ranks sum. This does not always agree in sign with a sign difference.
[b] Constrained fit: $5\geq\alpha\geq 0$, $2\geq\beta\geq\gamma\geq 0$ for $C(t)=K\left(\alpha e^{-\beta t}+e^{-\gamma t}\right)$.
[c] Constrained fit: $\beta\geq 0$ for $C(t)=K\,t^{\alpha-1}e^{-\beta t}$

007

CROSSED CEREBELLAR DIASCHISIS ON F18-FDG CEREBRAL TEP IN CHILDRENS WITH EPILEPSY.

Sophie TURPIN, MD*; Raymond Lambert MD*; Paola Diaodiri MD**; Anne Lortie MD **; Lionel Carmand MD**
.* Department of Nuclear Medicine, .** Department of Neurology, Hopital Ste Justine , Montreal, Canada

The purpose of the study was to evaluate the occurrence of crossed cerebellar diaschisis on F18-FDG cerebral TEP scan in childrens with epilepsy.
39 F18-FDG TEP studies performed in 37 patients were retrospectively reviewed. Patients with significant anatomical abnormalities were excluded. Most of the patients presented themselves with either frontal or temporal epilepsy. Regions of hypo and hypermetabolism and their localisation were searched for = and the presence or absence of either crossed cerebellar diaschisis or inverted crossed cerebellar diaschisis. Findings were correlated with clinical datas (suspected seizure origin).
F18-FDG TEP studies were normal in 11 cases.
In 7 studies, diffuse hemispheric decreased activity was found and crossed cerebellar diaschisis in 2 (1 frontoparietal suspected epileptic focus and 1 temporal).
In 15 studies, focal decreased activity was found. In 8, decreased activity involved the frontal regions, in patients with suspected frontal epilepsy and there was 2 cases of crossed cerebellar diaschisis. In 7, decreased activity involved posterior cerebral regions, in patients with suspected temporal or occipital epilepsy. There was no cases of crossed cerebellar diaschisis.
Some patients had ictal F18-FDG TEP studies due to the multiplicity and recurrence of their crisis or a status epilepticus. Focal increased activity was found in 6 studies. In 5 cases, increased activity was in the frontal region, and 1 had inverted crossed cerebellar diaschisis.

Crossed cerebellar diachisis is not infrequent in childrens with epilepsy and its presence suggest a frontal origin. In patients with multiples seizures, inverted crossed cerebellar diaschisis can be observed.

008

RADIATION EXPOSURE TO A FAMILY MEMBER IN THE INJECTION ROOM DURING DOSE ADMINISTRATION

Catherine M. Henderson, Dawn N. Burkhardt
Department of Nuclear Medicine, University Hospital, Indiana University Purdue University, Indianapolis, Indiana 46202

Often a family member accompanying a patient during the nuclear medicine procedure comes into the injection room to support the patient during their procedure. This study evaluated the safety of the accompanying patient's family member by determining the radiation exposure they might have received if present in the injection room. Within the medical community, imaging using ionizing radiation has become imperative for diagnosing and treating diseases. When an individual is in the area of a radioactive source, there are possible health risks involved. The goal of this study was to determine if the patient's family member would receive significant radiation exposure.
Exposure rates were measured with an electronic pocket Geiger Muller dosimeter. The dosimeter was placed one and a half meters away from the injection area. Background was recorded and was consistent with one working day. Readings from the dosimeter were recorded daily for fifteen days. The procedure, isotope, dose administered, and time in the room were recorded when a dose administration occurred within the injection room. Out of the fifteen days, only two days went above background level. On these two days I-131 thyroid therapy doses were given. When comparing the mean exposure to the maximum radiation exposure limit for the general public of 1 mSv (p-value less than 0.001), the data was significantly lower than this set limit. Comparing the mean exposure to background activity, the data was equivalent to background.
Radiation exposure readings to family members did not exceed background levels unless I-131 therapy was administered.

009

CAN NEUROSPECT BE HELPFUL IN ASSESSMENT OF POST TRAUMATIC SMELL IMPAIRMENT?

F. Abbaspour[1], H. Gerami[2], H. Bagheri[2];
1. Morvarid gamma scan center, Nuclear medicine department, Baran Physician Building, 76 Ave., Golsar Blvd., Rasht, Iran Tel:+98-131-7221816 Email: farzad_abbaspour@yahoo.com 2. Guilan university of medical sciences, ENT department, Rasht, Iran

Objectives: Smell impairment is a complication on post traumatic patients. Since most olfactory testing are subjective and depend upon the patient's response, they can conduct to false positive results. The aim of this study was to use quantitative brain perfusion SPECT in order to detect possible areas of brain activation in response to odorant stimulation in patients with post-traumatic anosemia comparing to a control group.
Methods used: Nineteen patients with post-traumatic impaired smell (anosemic) and 13 healthy controls were entered in this prospective study. All subjects underwent brain SPECT after IV injection of 740-MBq 99mTC-ECD and 48 hours later, the same procedure was repeated following olfactory stimulus by vanilla powder. Eight ROI were defined on sagittal slices (orbital frontal cortex, Inferior frontal pole, superior frontal pole, posterior superior frontal lobe, parasagittal area, occipital pole, Cerebellar and Cerebral area).
Results obtained: We compared the orbitofrontal area to cerebral ROI on before and after olfactory stimulation images on both patients and control group. Control group shows a more significant increase than patients in count of orbitofrontal lobe comparing to cerebral ROI in both hemispheres. In control group P value was <0.0001 on both hemispheres and in patients right and left ROI were <0.031 and <0.005 respectively.

Conclusions: Brain SPECT can be helpful in assessment of patients with post traumatic anosemia and could provide competitive data to other imaging techniques, especially when other modalities such as functional MRI is unavailable . However, this procedure may benefit from subjective tests, MRI or CT imaging.

010

COMPARATIVE STUDY OF ^{64}CU LABELLED DOTA- AND NOTA-FUNCTIONALIZED PEPTIDES FOR BREAST CANCER PET IMAGING

Fournier, Patrick, Dumulon-Perreault, Véronique, Ait-Mohand, Samia, Tremblay, Marie-Claude, Bénard, François and Guérin, Brigitte.

Objectives: The aim of this study was to compare ^{64}Cu labelled DOTA- and NOTA-functionalized peptide radiotracers targeting gastrin releasing peptide receptors (GRPR) and neuropeptides Y1 receptors (NPY1R) for breast tumor imaging by PET.
Methods: All peptides were synthesized on solid phase using the Fmoc strategy. Competitive binding assays were performed on human breast cancer cell lines (T47D and MCF-7) to estimate the inhibition constants (Ki) for both receptors. Peptides were labelled with ^{64}Cu following an approach proposed by Chen et al. (J Nucl Med **2004**; 45:1390) or using microwave. Plasma stability studies were achieved by incubating ^{64}Cu-labelled peptides (5 mCi) at 37°C in 150µL of fresh mouse serum for 1h. Stability was assessed by reversal phase HPLC using a radiometric detector. The cell uptake and internalization studies were performed for 15, 30, 60 and 90 minutes on T47D cells in contact with 0,3 µCi of radiolabelled peptides. The percentages of added dose by 10^5 cells (%AD/10^5 cells) bound and internalized were determined using a Cobra II auto-gamma counter.
Results: NOTA-peptides showed higher affinities for their receptors than the DOTA-peptides. HPLC analysis after a 1h incubation in mouse plasma showed no degradation or decomplexation of radiolabelled ^{64}Cu/DOTA- and ^{64}Cu/NOTA-BBN(6-14) peptides targeting GRPR. However, for peptides targeting NPY1R, only 15% and 32% of ^{64}Cu/DOTA- and ^{64}Cu/NOTA-(Lys^4)BVD15 were respectively recovered when incubated under the same conditions. The cell uptakes were respectively 0,93±0,46 and 1,52±0,09 %AD/10^5 cells for DOTA- and NOTA-BBN(6-14) derivatives.
Conclusion: NOTA is a more appropriate chelator for peptide radiolabelling with ^{64}Cu offering better affinity, plama stability, cell uptake and internalization. The positioning of the NOTA affects the results obtained.

011

BRACHIAL HYPEREMIC REACTIVITY KINETICS: A MULTIVARIATE BIOMARKER OF CORONARY ARTERY DISEASE CORRELATED WITH MAJOR CARDIOVASCULAR RISK FACTORS.

XueLi Zhao, PhD[1,2,3], Simon L. Bacon PhD[2,3,4,5] Jocelyn Dupuis, MD, PhD[6], Bernard Meloche NMTcn[1,2,3], Kim L. Lavoie PhD [2,3,5,7], André Arsenault, MD[1,2,3,6]

Background: A multivariate kinetic biomarker of CAD was derived from a two-compartment model of tetrofosmin forearms uptake following unilateral brachial hyperemic reactivity challenge (BHR). It was used to discriminate CAD patients from low-risk individuals. The predictive ability of BHR was compared to Framingham and Reynolds scores and the correlation with major cardiovascular risk factors was explored.
Methods and results: 46 confirmed CAD and 47 low risk participants were analyzed. A two-compartment model of blood and muscle kinetics was fitted to both forearms time activity curves. Six predictors were identified by discriminant analysis and the kinetic multivariate canonical score (biomarker) was saved for ROC curve analysis. Each predictor was tested by GLM taking all others as covariates also including major risk factors. The correlation between risk factors and the six parameters including the biomarker was assessed. The biomarker predicted groups with a sensitivity of 0.87, a specificity of 0.83, and an area under the ROC curve of 0.88. Five of the

parameters showed significant differences between groups after covariate adjustment. The ROC curve of the kinetic biomarker (0.88) compared favorably with Framingham and Reynolds scores of 0.68 and 0.76 respectively and showed a significant link with age, BMI, systolic blood pressure, HDL, triglycerides, and glucose levels.
Conclusions: The biomarker derived from forearm kinetic analysis of BHR is a powerful indicator of the presence of CAD. The six parameters differentially relate to major cardiovascular risk factors. This improved method could be an effective tool for risk stratification, detection, prevention and treatment response.
[1] Sygesa Ltd ; [2] Montreal Heart Institute; [3] Montreal Behavioural Medicine Centre; [4] Department of Exercise Science, Concordia University ; [5] Research Centre, Hospital du Sacre-Coeur de Montreal ; [6] Department of Medicine, Montreal Heart Institute; [7] Department of Psychology, University of Quebec at Montreal (UQAM).

Eric Lepp Clinical Vignettes

EL-001

INFECTIVE ENDOCARDITIS OF PROSTHETIC AORTIC VALVE WITH SPLENIC ABSCESS DETECTED ON FDG PET/CT

Authors: Abikhzer, Gad MDCM, Rush, Chris MDCM, FRCPC, Lipes, Jed MDCM, FRCPC.
Department of Nuclear Medicine, Jewish General Hospital, McGill University,

An 82 year old male presented to the emergency room with 2 months of progressive fatigue, myalgia, memory impairment and fever. He was previously known for diabetes, coronary artery bypass surgery as well as a bioprosthetic aortic valve replacement 2 years previously. He had been previously evaluated for the above symptoms as an outpatient and was treated empirically with prednisone for a presumptive diagnosis if polymylagia rheumatica. After a few weeks of treatment he failed to improve and subsequent evaluation revealed anaemia and a hypodense splenic lesion on CT, suspicious for lymphoma. An FDG PET/CT was performed to assess the splenic lesion. While awaiting the results, he presented to the emergency department with presyncope, and fever.
There was intense FDG uptake in the aortic valve prosthesis. The hypodense splenic mass on CT demonstrated no FDG uptake in the center of the lesion and a thin rim of faint hypermetabolic activity. Based on these findings, the FDG PET was interpreted as compatible with an infected prosthetic aortic valve with a splenic abscess due to showering of septic emboli. Blood cultures in the ER quickly grew 4 /4 bottles of penicillin sensitive streptococcus viridians and an echocardiogram was performed revealing global LV dysfunction with an EF of 45%, moderate mitral regurgitation with thickened mitral leaflets and anterior mitral valve prolapse. The aortic root appeared thick as well. A first attempt at a transesophageal echocardiography was done but could not be completed as the probe could not pass through the esophagus. Given the FDG PET findings, a second attempt at a TEE with a pediatric probe revealed a 5x6 mm vegetation on the anterior mitral leaflet with evidence of anterior leaflet perforation as well as a thickened BioAVR. The aortic root showed a 19x9 mm area of echolucency which combined with the FDG findings was suggestive of aortic root abscess. Imaging of the brain revealed multiple embolic CNS infarcts. The patient was therefore diagnosed with subacute bacterial endocarditis with embolization to his brain and spleen. Due to his frail state and high operative morbidity and mortality, a decision was made to treat the endocarditis with medical management. He completed 3 months of therapy with Penicillin G without further embolic events and had some modest improvement in function and was discharged from hospital in stable condition. The FDG PET/CT revealed the source of his FUO, guided directed imaging and allowed for the appropriate treatment and therefore survival of this patient.

EL-002

^{18}F FDG PET/CT IN THE MANAGEMENT OF AIDS COMPLICATIONS

Abikhzer, Gad MDCM, Derbekyan, Vilma MDCM, FRCPC, Hickeson, Marc MDCM, FRCPC.
Department of Nuclear Medicine, Royal Victoria Hospital, McGill University

A 40 year old HIV positive male presented with clinically apparent underwent lymphadenopathy and hepatosplenomegaly. A PET/CT was performed for the evaluation of a suspected lymphoma. The scan showed multiple hypermetabolic lymph nodes in the cervical, supraclavicular, axillary, mediastinal, paraesophageal, and intraabdominal lymph node stations. There is also evidence of hepatosplenomegaly. A biopsy of the esophagus showed evidence of herpes esophagitis. A biopsy of a right axillary lymph node showed regressive transformation of a few germinal centers, consistent with Castleman's disease, plasma cell variant. Subsequent follow up FDG PET scans after therapy showed resolution of the FDG uptake in the lymph nodes, compatible with a favorable response to treatment. There was however, intense hypermetabolic activity in the distal third of the esophagus. A biopsy of the esophagus showed evidence of herpes esophagitis. Thus, in a patient with AIDS, there may be multiple complications that can be diagnosed on a FDG PET study. This case illustrates that in addition to multicentric Castleman's disease the patient later developed a second AIDS related complication, herpes esophagitis. FDG PET can be used to guide biopsy sites to differentiate between lymphoma from infectious complications of AIDS. It can also be used to follow up response to therapy.

EL-003

^{18}F FDG PET/CT IN THE MANAGEMENT OF DISSEMINATED HISTOPLASMOSIS

Abikhzer, Gad MDCM, Derbekyan, Vilma MDCM, FRCPC.
Department of Nuclear Medicine, Royal Victoria Hospital, McGill University

A 31 year old female patient presented with neck adenopathy and B symptoms consisting of significant weight loss and night sweats. Lactate Dehydrogenase (LDH) level was high at 500 U/L. A FDG PET/CT scan was done to evaluate for the presence of lymphoma. An HIV test was also sent and the patient was confirmed to be HIV positive with a high viral load of 171880 copies/ml. The PET/CT showed multiple hypermetabolic lymph nodes on both sides of the diaphragm as well as abnormal focal hypermetabolism in the stomach, colon and left adrenal gland. The findings can certainly be due to lymphoma but an infectious etiology was on the differential given the HIV status of the patient. A biopsy of one of the neck nodes showed evidence of necrotizing granulomatous inflammation with fungal organisms identified in the sample, consistent with a diagnosis of histoplasmosis. An endoscopic biopsy of the stomach was also consistent with histoplasma capsulatum infection. Non-invasive candida was also present on the tissue sample from the stomach. No histopathological diagnosis is available on the left adrenal gland findings. Although the patient presented with classical symptoms of lymphoma as well as imaging findings compatible with lymphoma, the patient was diagnosed with acquired immune deficiency syndrome (AIDS) and a disseminated histoplasmosis infection. The role of PET/CT in such cases is to aid in the accurate localization of metabolically active disease to determine appropriate biopsy sites. Interpreters need to be aware of diseases that can mimic the appearance of lymphoma on FDG PET/CT.
